Biomaterials Science

PAPER

View Article Online
View Journal | View Issue

Cite this: *Biomater. Sci.*, 2014, **2**, 1110

Incorporating the BMP-2 peptide in genetically-engineered biomaterials accelerates osteogenic differentiation†

Yeji Kim,[a] Julie N. Renner[a] and Julie C. Liu*[a,b]

Received 25th December 2013,
Accepted 21st March 2014

DOI: 10.1039/c3bm60333d

www.rsc.org/biomaterialsscience

Protein-based biomaterials have emerged as powerful tools for tissue engineering applications. Recombinant DNA techniques can be used to precisely tune material properties at the molecular level, and multiple peptide modules can be incorporated into a single material. Here, we genetically engineered biomaterials that incorporate a peptide derived from bone morphogenetic protein-2 (BMP-2) and investigated whether the BMP-2 peptide, within the context of these materials, can promote stem cells to produce bone matrix and synergize with a cell-binding sequence (RGD). Our study is the first to demonstrate that when the BMP-2 peptide is incorporated within the backbone of protein-based biomaterials, it is active and accelerates osteogenic differentiation of mesenchymal stem cells. In particular, cells seeded on proteins containing the BMP-2 peptide had increased levels of alkaline phosphatase (AP) activity, calcium deposition, and expression of bone-related genes. However, the BMP-2 peptide did not synergize with the RGD cell-binding domain within the context of these protein-based materials. Overall, these results suggest that incorporation of the BMP-2 peptide within the context of modular proteins is a successful strategy for engineering biomaterials for applications in bone tissue engineering.

Introduction

Protein-based biomaterials have emerged as promising tissue-engineered scaffolds. These materials, whose peptide sequences are precisely tuned at the molecular level, can be manufactured *via* solid-phase peptide synthesis (SPSS) or genetic engineering.[1] SPSS is a rapid method to produce short peptides (*i.e.*, 35–40 amino acids).[2] Compared to SPSS, genetic engineering allows researchers to create peptides and proteins with a wide range of sizes. In addition, the longer length of biomaterials produced by genetic engineering allows for facile incorporation of multiple functionalities through sequences such as structural (*i.e.*, structural motifs or crosslinking sites) and bioactive domains (*i.e.*, biochemical factors). For example, recent studies have utilized elastin-like,[3–6] resilin-like,[7–9] and silk-like sequences[10,11] as structural domains to provide mechanical properties suitable for specific tissue engineering applications. In addition, cell-binding sequences,[9,12,13] heparin-binding sequences,[14] and matrix metalloproteinase degradation sites[7] have been incorporated as bioactive domains to elicit desired cellular responses.

In particular, bioactive domains, such as cues to promote stem cell differentiation, that are incorporated directly into protein-based biomaterials act as material-based cues and have a number of advantages over soluble cues. Material-based cues remain at the target site, whereas soluble growth factors can diffuse away from the target and result in off-target effects. Thus, material-based differentiation cues would lead to more uniform differentiation compared to soluble cues, which could result in diffusion gradients and heterogeneous differentiation. In addition, soluble cues often are utilized at supra-physiological concentrations, which causes side effects.[15] In contrast, attaching a cue to the material has the potential to lower the overall concentration by effectively increasing the local surface concentration. Furthermore, differentiation cues such as growth factors are often bound to the extracellular matrix, and material-based cues mimic this mode of presentation.

This study investigates the use of material-based cues within the context of modular proteins that are designed to promote stem cells to produce bone matrix. Our modular proteins were designed to contain a resilin-like structural domain and a bioactive domain (Fig. 1). Our previous work demonstrates that similar materials are cytocompatible and that when the RGD cell-binding domain was incorporated within

[a]*School of Chemical Engineering, Purdue University, West Lafayette, IN 47907, USA*
[b]*Weldon School of Biomedical Engineering, Purdue University, West Lafayette, IN 47907, USA. E-mail: julieliu@purdue.edu; Fax: +1-765-494-0805; Tel: +1-765-494-1935*
† Electronic supplementary information (ESI) available. See DOI: 10.1039/c3bm60333d

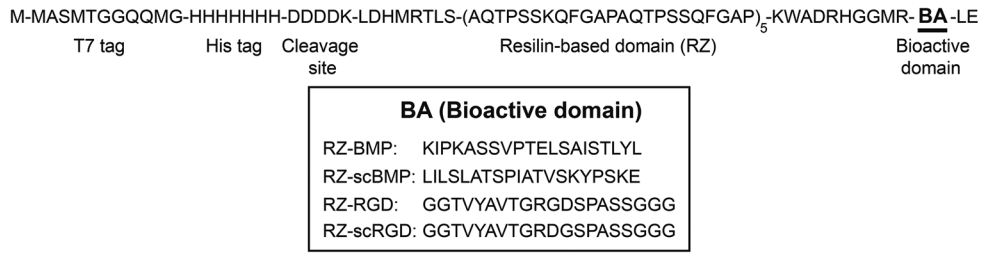

Fig. 1 The full amino acid sequences of modular proteins used in this study. At the N-terminus, each protein has a T7 tag for protein identification, a heptahistidine tag (His tag) for identification or purification, and an enterokinase cleavage site for removal of the tags from the modular proteins. The bioactive domain (BA) (indicated by a black bar) contains one of the sequences listed in the box. For example, the bioactive domain of the RZ-BMP protein includes the BMP-2 peptide sequence, KIPKASSVPTELSAISTLYL. The RZ-scBMP and RZ-scRGD proteins serve as sequence-scrambled negative control proteins.

the protein-based materials, it promoted a faster rate of cell spreading compared to the sequence-scrambled negative control protein.[9] In the current work, we focus on incorporating a peptide sequence derived from bone morphogenetic protein-2 (BMP-2) growth factor and examining the ability of this modular protein to induce osteogenic differentiation.

Human mesenchymal stem cells (hMSCs) derived from the bone marrow have been extensively used in the field of tissue engineering because they are able to differentiate into multiple lineages such as bone, cartilage, muscle, and fat.[16] BMP-2 growth factor is one of the most common cues for promoting differentiation of hMSCs into osteogenic lineages. It has been widely studied *in vitro* and *in vivo* in applications of bone tissue engineering and is being used clinically for bone regeneration.[17]

A short peptide sequence derived from the knuckle epitope of BMP-2 (hereafter referred to as the BMP-2 peptide) was synthesized and shown to have bioactivity similar to the full-length BMP-2 growth factor; the peptide specifically bound to two types of BMP receptors.[18] Further studies demonstrated that incorporating the BMP-2 peptide in biomaterials induced osteogenic differentiation and ectopic bone formation[19–23] and *in vivo* bone regeneration.[24,25] In addition, there was a synergistic effect on osteogenic differentiation when the BMP-2 peptide and the RGD cell-adhesion sequence were both incorporated into scaffold materials.[20,26,27] Thus, these studies demonstrated that the BMP-2 peptide was active when incorporated within biomaterials, but these studies were limited to immobilizing or grafting the sequences on the materials.

Here, we expand the utility of the BMP-2 peptide by demonstrating that it is bioactive within a new mode of ligand presentation (*i.e.*, within the context of a genetically-engineered biomaterial). In particular, we utilize genetic engineering to incorporate the BMP-2 peptide directly into the backbone of our protein-based materials. Thus, the goal of this study was to investigate the ability of the BMP-2 peptide to promote osteogenic differentiation of hMSCs when presented within the context of the backbone of our genetically-engineered biomaterials. To accomplish our goal, we first used recombinant protein engineering to incorporate the BMP-2 peptide in modular proteins. Next, we evaluated the metabolic activity of human MSCs on our proteins. Last, we investigated whether genetically-engineered biomaterials incorporating the BMP-2 peptide enhanced osteogenic differentiation and whether there were synergistic effects with the RGD cell-binding domain.

Materials and methods

Materials

All materials used in this study were purchased from Sigma-Aldrich unless stated otherwise.

Material design

The DNA constructs were cloned using the methods previously described.[28] In this study, the proteins consisted of ten repeats of a resilin-like sequence (RZ) derived from *Anopheles gambiae* and a bioactive domain (BA). The sequences for the BA domain are listed in Fig. 1.

Protein expression and purification

Protein expression was performed as previously described.[9] Briefly, *E. coli* strain BL21-CodonPlus (DE3)-RIPL (gift from Dr. Jo Davisson, Purdue University) containing the desired recombinant plasmid was inoculated in medium containing 35 μg mL^{-1} kanamycin and 34 μg mL^{-1} chloramphenicol. Small-scale protein expression was conducted in 4 L baffled flasks, whereas large-scale protein expression was performed in a fermentor (BioFlo 110, 14 L capacity, New Brunswick). Expression was induced with isopropyl β-D-1-thiogalactopyranoside (IPTG, Denville Scientific).

Proteins were purified by a salting-out and heating method as previously described.[9,28] Briefly, cell pellets were resuspended in 8 M urea (pH 8.0), and cells were lysed using freeze–thaw cycles and sonication. After salting out undesired proteins, the modular proteins were precipitated with 20 (w/v)% ammonium sulfate. The re-suspended proteins were heated at 80 °C for 10 min to remove undesired proteins. The solution was then dialyzed and freeze-dried.

The molecular weight and purity of proteins were confirmed by sodium dodecyl sulfate-polyacrylamide gel electrophoresis (SDS-PAGE) analysis. Protein purity was determined

by densitometry analysis using Image J software (NIH). The composition of purified proteins was confirmed by amino acid analysis (Purdue Proteomics Facility at the Bindley Bioscience Center). The bioactive domain sequences of the RZ-RGD and RZ-scRGD proteins were confirmed by peptide sequencing (Purdue Proteomics Facility at the Bindley Bioscience Center). Briefly, the proteins were digested with endoproteinase AspN, and the fragments were sorted by mass. Fragments from the C-terminus containing the last 11 (RZ-RGD) or 12 (RZ-scRGD) amino acids were further fragmented into smaller pieces to determine each amino acid sequence.

Surface preparation

Protein surfaces were prepared 24 h before cell seeding. Proteins were dissolved in phosphate-buffered saline (PBS) at 1 mg mL^{-1} and adsorbed on tissue culture polystyrene (TCP) at 4 °C overnight. The next day, the surfaces were washed with PBS three times to remove unbound proteins. Surfaces were blocked with 0.2 (w/v)% bovine serum albumin (BSA) (fraction V) that had been heat-inactivated at 85 °C for 10 min. Blocking was performed for 30 min at room temperature, and then the surface was rinsed with PBS three times. The density of the proteins adsorbed on TCP was determined before cell differentiation studies (Fig. S1†).

Cell culture

To investigate cell responses on the proteins, hMSCs (Lonza) were cultured at 37 °C and 5% CO_2 in growth medium consisting of low-glucose Dulbecco's modified Eagle's medium (DMEM) supplemented with 10% fetal bovine serum (Lonza), 100 U mL^{-1} penicillin, 100 mg mL^{-1} streptomycin (Invitrogen), and 10 ng mL^{-1} basic fibroblast growth factor (bFGF, R&D Systems, courtesy of the National Cancer Institute Preclinical Repository). Cells were seeded at a density of 5000–6000 cells cm^{-2} and sub-cultured after they reached 60–80% confluence.

To investigate the bioactivity of our proteins, hMSCs were seeded at a density of 3100 cells cm^{-2} on TCP or proteins. After the cells reached 70–85% confluence, they were cultured in osteogenic medium consisting of growth medium without bFGF and supplemented with 100 nM dexamethasone, 50 μM ascorbic acid 2-phosphate, and 10 mM glycerol-2-phosphate disodium salt hydrate. The medium was replaced every three days. All experiments were performed using cells at passages 3–5.

Cellular metabolic activity

Cellular metabolic activity on proteins was measured by monitoring the reduction of the tetrazolium salt WST-1 (GBioscience). Briefly, 10 μL of the reagent was added to each well containing 100 μL of the growth medium, and cells were incubated for 4 h at 37 °C. The absorbance of the medium was measured at 440 nm by a SpectraMax M2^e (Molecular Devices) and normalized by the absorbance reading at 600 nm. At each time point, metabolic activity was determined as the percentage relative to the positive control (cells on TCP). Six replicates per group were examined.

Alkaline phosphatase (AP) activity

Culture medium was replaced 24 h prior to cell lysis to prevent serum starvation. Cells were washed with PBS once and lysed in 0.1 (v/v)% triton in water (pH 7.4) for 15 min at room temperature. Collected cells were frozen at −80 °C before being assayed. Frozen cells were thawed and centrifuged, and the supernatant was collected. For DNA quantification, 50 μL of Hoechst 33 258 solution (0.7 μg mL^{-1} in 50 mM Tris, 100 mM NaCl, and 0.1 mM EDTA, pH 7.4) was mixed with an equal amount of the supernatant, and the fluorescence was measured with an excitation at 340 nm and emission at 465 nm. Calf thymus DNA was used as a standard. For assessment of AP activity, 50 μL of the supernatant was combined with 50 μL of *p*-nitrophenol phosphate solution (10 mg mL^{-1} in 0.1 M glycine and 1 mM $MgCl_2$, pH 9.6) and incubated at 37 °C for 150 min. The absorbance was measured at 405 nm, and *p*-nitrophenol (Alfa Aesar) was used as a standard. AP activity was normalized by the amount of DNA and incubation time. Three or four replicates of each group were examined.

Calcium deposition

At each time point, cells were fixed with 4 (w/v)% paraformaldehyde in PBS at room temperature for 15 min and then washed with Milli-Q water (Millipore) three times. Cells were stained with 40 mM Alizarin red S (pH 4.1) for 40 min at room temperature with gentle shaking. After Alizarin red S staining, cells were washed with Milli-Q water five times to remove excess dye. The plates were stored at −20 °C until imaging and dye extraction. All images were obtained at the same time by using a 4× objective on a Nikon Ti-EC-1 Plus microscope.

Calcium deposits were quantified by extracting Alizarin red S from the stained monolayer as previously described.[29] Briefly, stained cells were incubated with 10 (v/v)% acetic acid for 30 min with gentle shaking. The cell solution was heated at 85 °C for 10 min and then incubated on ice for 5 min. Following centrifugation, the supernatant was neutralized with 1 (v/v)% ammonium hydroxide to adjust the pH between 4.1 and 4.5. The total amount of extracted dye was determined by measuring the absorbance at 405 nm. Alizarin red S solutions in acetic acid (pH 4.1–4.5) were used as a standard. Three to six replicates per group were examined.

Quantitative reverse transcription-polymerase chain reaction (qPCR)

The medium was replaced 24 h before sample collection to prevent serum starvation. Samples were processed and analyzed as previously described.[30] After removal of genomic DNA, the amount of purified RNA was measured on a Nanodrop spectrophotometer (ND 1000, Thermo Scientific). At least 0.5 μg RNA was used to produce complementary DNA. For qPCR, all individual samples were run in duplicate (day 7 and 11) or triplicate (day 4). The primer sequences for runt-related transcription factor 2 (Runx2), AP, type I collagen (type I col), osteopontin (OPN), bone sialoprotein (BSP), type II collagen (type II col), and glyceraldehyde-3-phosphate dehydrogenase

(GAPDH) were obtained from references or designed using Primer-Blast on the National Institutes of Health website (Table S1†). The relative gene expression level was calculated by the ΔΔCt method; GAPDH was used as the housekeeping gene, and expression levels were determined relative to the positive control (TCP). There were four to six replicates per group.

Statistical analysis

All data are represented as mean ± standard deviation. Normality and homogeneity of variance were confirmed by Shapiro–Wilk and Levene's modified tests, respectively. For data that passed both tests, one-way analysis of variance (ANOVA) was performed. Dunnett's test was performed at each time point to determine significant differences between the control (TCP) and an experimental group. Statistical differences between experimental groups were also determined by Tukey's *post hoc* test. Data showing unequal variances (days 9 and 11 in Fig. 4) were analyzed by a Box-Cox transformation.[31] Data with a non-normal distribution (day 9 in Fig. 5B) were evaluated by a non-parametric Kruskal–Wallis test. All statistical analyses were performed using Statistical Analysis Software (SAS, version 9.2), and values of $p < 0.05$ were considered to be statistically significant.

Results

Material design, production, and characterization

The full amino acid sequences of proteins used in this study are shown in Fig. 1. Each protein consists of a structural domain to provide mechanical integrity and a bioactive domain to promote cell differentiation. Ten repeats of a resilin-like consensus sequence (RZ) derived from *A. gambiae*, AQTPSSQYGAP, comprised the structural domain. The bioactive domain included either the BMP-2 peptide (RZ-BMP proteins) or the cell-binding sequence (RZ-RGD proteins). Proteins containing scrambled versions of the BMP-2 peptide (RZ-scBMP proteins) or the cell-binding sequence (RZ-scRGD proteins) served as negative control proteins whose amino acid composition matched those of the RZ-BMP and RZ-RGD proteins, respectively. Our previous work describes the manufacture and initial characterization of the RZ-RGD and RZ-scRGD proteins.[9] Thus, this work will describe the production and initial investigation of the RZ-BMP and RZ-scBMP proteins.

The average yields of purified RZ-BMP and RZ-scBMP proteins in small- and large-scale expressions were 10 and 27 mg per liter of culture, respectively. SDS-PAGE analysis confirmed that the RZ-BMP and RZ-scBMP proteins ran near the expected molecular weight of 18.6 kDa and that the proteins were >90% pure (Fig. 2). Amino acid analysis confirmed the compositions of the RZ-BMP and RZ-scBMP proteins, and the observed value of each component was within 1 mol% of the anticipated value (Table S2†). Circular dichroism (CD) spectroscopy demonstrated that the RZ-BMP and RZ-scBMP proteins have an unordered structure (Fig. S2†), which is similar to the structure of the RZ-RGD and RZ-scRGD proteins previously reported.[9]

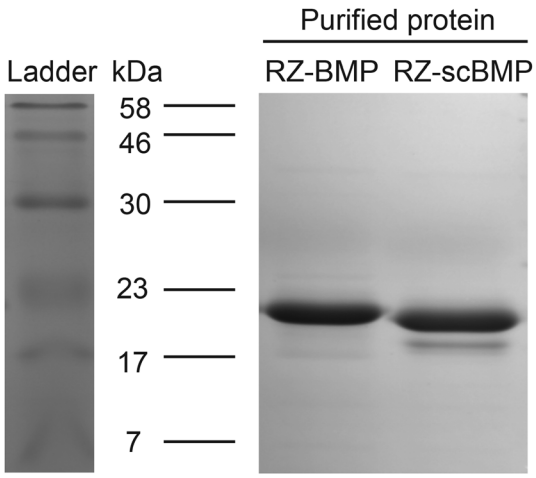

Fig. 2 Successful purification of RZ-BMP and RZ-scBMP proteins. Proteins were analyzed on an SDS-PAGE gel and appeared close to the expected molecular weight of 18.6 kDa. Densitometry analysis confirmed that the protein samples were ≥90% pure.

Human MSC metabolic activity on modular proteins

Cellular metabolic activity on proteins was assessed by the WST-1 assay (Fig. 3). After one day of seeding, it appeared as if fewer cells had attached to our protein surfaces compared to TCP. In particular, the number of hMSCs on RZ-BMP and RZ-scBMP proteins was 71 ± 11 and 71 ± 6%, respectively, compared to those on the positive control (TCP). However, 2–4 days after seeding, there was no difference in the metabolic activity of cells grown on TCP or the proteins. These results suggest

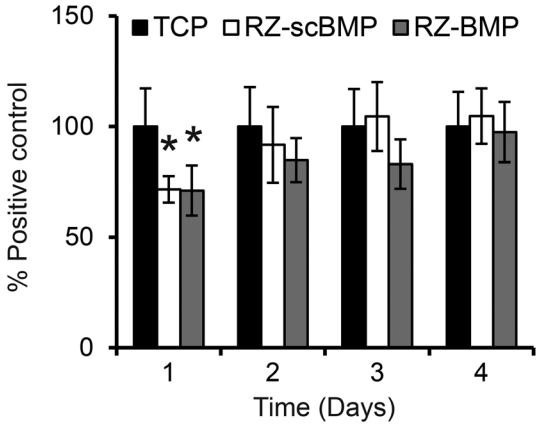

Fig. 3 Human MSC metabolic activity on the RZ-BMP and RZ-scBMP proteins. At each time point, cellular metabolic activity was evaluated by the WST-1 assay, and the results are presented relative to the positive control (TCP). Cells on all three surfaces had statistically equivalent metabolic activity 2–4 days after seeding. These results suggest that the RZ-BMP and RZ-scBMP proteins supported cell proliferation. Data are represented as the average ± standard deviation of six replicates. * indicates $p < 0.05$ compared to the positive control (TCP) at that time point as determined by Dunnett's test.

that the RZ-BMP and RZ-scBMP proteins are cytocompatible and support hMSC proliferation at a rate similar to TCP. In subsequent differentiation studies, differentiation medium was added 4 days after seeding, at which time cell number and metabolic activity were equivalent on all surfaces.

Presenting the BMP-2 peptide within the context of genetically-engineered proteins accelerates osteogenic differentiation

In examining cell differentiation on our proteins, our first objective was to determine whether incorporating the BMP-2 peptide within the context of protein-based biomaterials (RZ-BMP) would enhance osteogenic differentiation compared to control (TCP). Second, we evaluated whether there were synergistic effects when the BMP-2 peptide and the RGD sequence were individually incorporated within the backbone of the protein-based materials (RZ-BMP and RZ-RGD proteins, respectively). To accomplish this goal, we included two additional surfaces in our study – a 50 : 50 mixture of RZ-BMP and RZ-scRGD proteins (designated RZ-BMP + RZ-scRGD) and a 50 : 50 mixture of RZ-BMP and RZ-RGD proteins (designated RZ-BMP + RZ-RGD). To characterize cell response on proteins, we examined markers of osteogenic differentiation such as AP activity, calcium deposition, and gene expression levels.

AP activity, which is an early marker of osteogenic differentiation, was characterized by measuring the hydrolysis of *p*-nitrophenyl phosphate substrate (Fig. 4). At all time points, the AP activity of cells cultured on RZ-BMP was higher than on the positive control (TCP). Compared to TCP, the RZ-BMP proteins induced a 2-fold increase at early time points (4 and 7 days) and a 3-fold increase at later time points (9 and 11 days). However, cells cultured on the sequence-scrambled negative control RZ-scBMP protein did not enhance AP activity compared to cells on TCP. Of particular note, cells on RZ-BMP had statistically higher AP activity compared to cells on RZ-scBMP at all time points ($p < 0.05$, Tukey's *post hoc* test). Therefore, our results indicate that the RZ-BMP proteins effectively enhance AP activity in a sequence-specific manner.

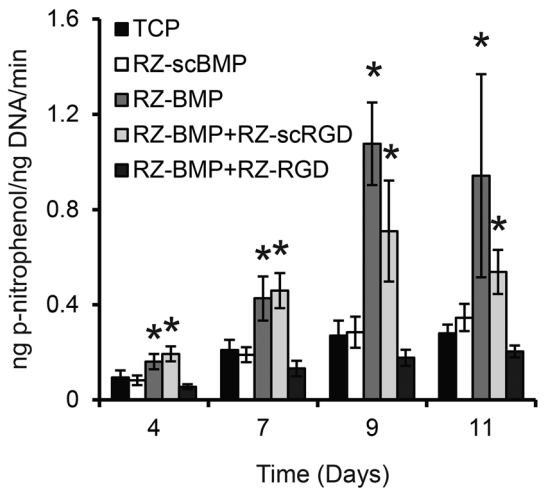

Fig. 4 Presenting the BMP-2 peptide within the context of genetically-engineered materials (RZ-BMP or RZ-BMP + RZ-scRGD proteins) enhances the AP activity of cells. Compared to cells on TCP, cells grown on RZ-BMP or RZ-BMP + RZ-scRGD proteins showed increased AP activity at all time points, whereas those on RZ-scBMP or RZ-BMP + RZ-RGD proteins did not. AP activity was normalized by the DNA amount and reaction time. Error bars indicate the standard deviation of 3–4 replicates. * indicates $p < 0.05$ compared to TCP at that time point as determined by Dunnett's test.

Cells on RZ-BMP + RZ-scRGD proteins had statistically higher AP activity compared to cells on TCP at all time points. Also, the AP activity of cells on RZ-BMP + RZ-scRGD was statistically equivalent to that of cells on RZ-BMP proteins ($p < 0.05$, Tukey's *post hoc* test). Interestingly, the AP activity of cells on RZ-BMP + RZ-RGD was not significantly different from those on TCP. Furthermore, from 4 to 9 days of differentiation, cells cultured on RZ-BMP + RZ-RGD showed a significantly lower AP activity than those on either RZ-BMP or RZ-BMP + RZ-scRGD ($p < 0.05$, Tukey's *post hoc* test).

Next, we carried out Alizarin red S staining to examine calcium deposition (mineralization) of cells cultured on the five different surfaces, and the extent of calcium deposition was quantified by extracting the dye from the stained monolayer (Fig. 5). After 9 days of differentiation, no mineralization was observed. However, the amount of calcium deposited increased from 9 to 11 days of differentiation. After 11 days of differentiation, cells cultured on RZ-BMP or RZ-BMP + RZ-scRGD exhibited a significant 3-fold increase in calcium deposition compared to those on TCP. However, the RZ-BMP + RZ-RGD proteins did not enhance calcium deposition.

Of note, cells grown on the RZ-scBMP proteins showed statistically higher calcium deposition than those on TCP at day 11. One possible reason for this response is that there was more RZ-scBMP adsorbed to the surfaces compared to RZ-BMP, RZ-BMP + RZ-scRGD, or RZ-BMP + RZ-RGD (Fig. S1B†). Due to the higher RZ-scBMP protein density, the increased number of non-specific interactions with the resilin portion or with the amino acids within the scrambled domain may have resulted in statistically higher calcium deposition on RZ-scBMP compared to TCP.

To ensure that our results can be attributed to protein surfaces and are not due to protein desorbing from the surface, we incubated the RZ-BMP surfaces with medium and used this pre-conditioned medium in cell differentiation studies. The medium pre-conditioned on the RZ-BMP proteins did not accelerate osteogenic differentiation compared to the medium pre-conditioned on TCP (Fig. S3†).

Finally, we examined the gene expression level of osteogenic markers by qPCR. Runx2 is a transcriptional factor involved in osteogenic lineage commitment, whereas AP and type I col are early- and mid-stage osteogenic markers, respectively. Compared to control (TCP), cells on RZ-BMP had higher expression levels of Runx2 at 11 days and type I col at 7 and 11 days (Fig. 6). Although the AP activity was elevated at all time points when cells were cultured on RZ-BMP (Fig. 4), no increases in gene expression of AP were observed (Fig. 6). Cells on the

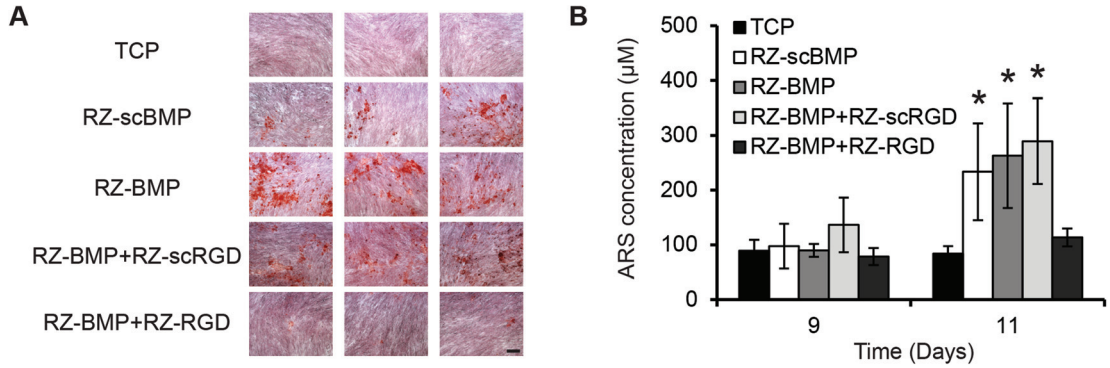

Fig. 5 Increased calcium deposition by cells grown on modular proteins. (A) Bright-field images of stained cell monolayers after 11 days of differentiation on TCP or the proteins. Cells were stained with Alizarin red S, and pictures from three separate wells are shown for each surface. Scale bar represents 250 μm. (B) Quantification of Alizarin red S (ARS) staining (n = 4–6) was performed by extracting dye from the stained monolayers. Compared to cells grown on TCP, cells on RZ-BMP and RZ-BMP + RZ-scRGD proteins showed increased calcium deposition at 11 days of differentiation. * indicates $p < 0.05$ compared to TCP at that time point as evaluated by Dunnett's test.

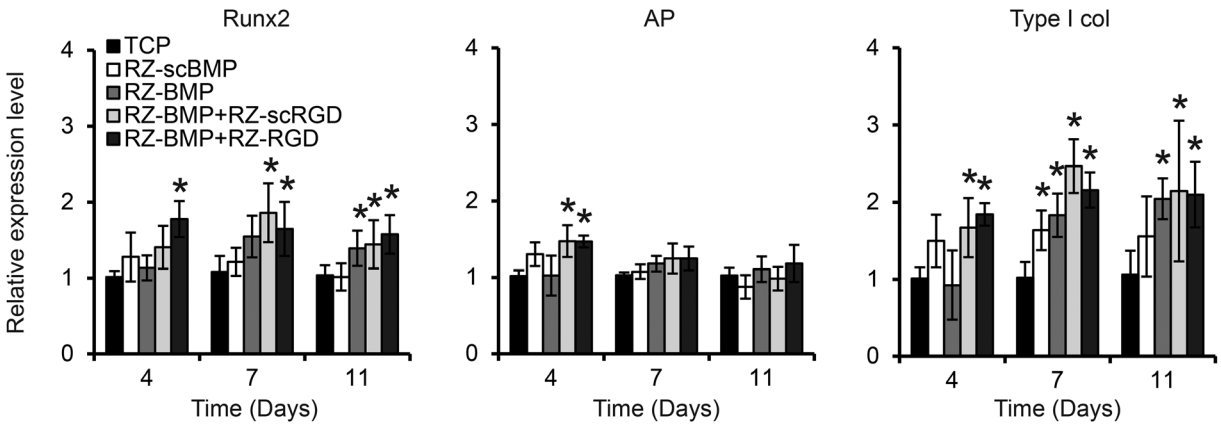

Fig. 6 Increased expression levels of bone-related genes by cells grown on modular proteins. Gene expression was measured by qPCR. The relative expression levels of Runx2, AP, and type I col of cells grown on TCP or the proteins were normalized by GAPDH (a housekeeping gene) and are reported relative to the control (TCP) at each time point. Data (n = 4–6) are represented as mean ± standard deviation. * indicates $p < 0.05$ compared to the positive control (TCP) at each time point as assessed by Dunnett's test.

RZ-scBMP proteins generally did not upregulate osteogenic markers except for the expression of type I col at 7 days.

The expression of Runx2 and type I col was enhanced on the RZ-BMP + RZ-RGD proteins at all time points compared to control (TCP). Furthermore, cells on RZ-BMP + RZ-RGD had increased AP levels on day 4. Cells on RZ-BMP + RZ-scRGD had responses similar to those on RZ-BMP + RZ-RGD except that Runx2 levels were not enhanced on day 4.

We also analyzed OPN and BSP, which are late markers of osteogenic differentiation, but no differences between groups were observed (Fig. S4†). To confirm whether cell differentiation on proteins is osteogenic-specific, we assessed the expression level of type II col, which is commonly associated with cartilage matrix. The type II col levels on all proteins were statistically equivalent at all time points (Fig. S4†), suggesting that cells are not undergoing cartilage differentiation.

Discussion

The full-length BMP-2 growth factor is a potent cue for promoting osteogenic differentiation and is approved by the Food and Drug Administration (FDA) to be used clinically to regenerate bone defects.[32] Despite the efficacy of the full-length BMP-2 growth factor on bone regeneration, its use in clinical applications in soluble form (*e.g.*, addition of soluble BMP-2, adsorption or encapsulation of BMP-2 in scaffold materials) is hampered by several factors. First, the production of recombinant human BMP-2 (rhBMP-2) is not yet cost-effective.[33] Mammalian cells result in low yields of rhBMP-2, and rhBMP-2 produced in bacteria (*i.e., E. coli*) is usually found in inclusion bodies, which complicates purification due to the additional steps of solubilization and refolding.[34,35] Second, the effective clinical concentration of soluble BMP-2 is often supra-physio-

logical (*e.g.*, several milligrams),[36] which causes adverse effects such as soft-tissue swelling[37] and inflammation.[38] Third, rhBMP-2 has a short half-life and retention time.[17]

An attractive alternative to using soluble full-length BMP-2 growth factor is to incorporate the short BMP-2 peptide,[18] which is known to promote bone regeneration, into a scaffold material. The shorter length reduces the production cost. Moreover, attaching the peptide to the material potentially lowers the overall concentration because of the increased local concentration and because the peptide does not diffuse away from the target site. This strategy has resulted in enhanced osteogenic differentiation and bone regeneration in biomaterials that present the BMP-2 peptide through covalent immobilization[20,21,23] or specific binding on the surface of the material.[19,24] However, none of these studies have explored directly incorporating the BMP-2 peptide within the material backbone and examined its bioactivity within the context of a genetically-engineered biomaterial.

Our approach enables multiple functionalities to be incorporated within the backbone of a single material. Because the amino acid sequence can be tightly controlled at the molecular level, genetic engineering allows us to precisely engineer materials to elicit desired cell responses.[1] In addition, given that the bioactive cues are incorporated into the backbone of the materials, our approach simplifies material preparation and characterization because it eliminates the additional steps needed to immobilize the cues on the material and quantify the ligand density.

Our modular proteins supported hMSC proliferation (Fig. 3), and the BMP-2 peptide in the modular proteins accelerated osteogenic differentiation compared to the control (TCP) (Fig. 4–6). When seeded on the RZ-BMP proteins, hMSCs showed higher levels of AP activity, calcium deposition, and gene expression of Runx2 and type I collagen compared to cells on TCP. Cells on RZ-BMP surfaces did not show higher AP gene expression than those on TCP. Given that mRNA is regulated upstream of protein translation and protein activity and that previous literature shows that AP expression levels are transient,[39,40] one potential reason for this discrepancy is that the time points we selected did not capture the transient increase in AP gene expression on RZ-BMP. In fact, AP enzyme activity on RZ-BMP surfaces was already elevated at day 4 in our results, and we postulate that AP gene expression on RZ-BMP may have increased and reached a peak prior to this time point. The pattern of AP gene expression peaking at an earlier time point than AP enzyme activity has been previously observed in literature.[41] The surface density of the BMP-2 peptide within the context of genetically-engineered biomaterials (69 ± 17 pmol cm^{-2}, Fig. S1B†) was similar to the density from previous studies when the peptide was grafted on materials (5.2–120 pmol cm^{-2} [20,26,42]). The bioactivity of the RZ-BMP proteins is likely to be osteogenic-specific, as there was no increase in the expression level of a cartilage marker (type II col) at all time points (Fig. S4†). Moreover, we confirmed that the bioactivity of the RZ-BMP proteins did not result from proteins desorbed from the plate (Fig. S3†). Thus, these results demonstrate the bioactivity of the BMP-2 peptide within the context of our modular proteins and the potential of our genetically-engineered biomaterials for accelerating osteogenic-specific differentiation.

The RZ-scBMP proteins, which serve as sequence-scrambled negative control proteins, increased a couple of osteogenic markers. Specifically, calcium deposition at day 11 and gene expression of type I collagen on day 7 were increased compared to TCP. We hypothesize that these effects may be due to the higher protein density of RZ-scBMP compared to other proteins (Fig. S1B†). In fact, several experiments which sought to use the same density of RZ-BMP and RZ-scBMP confirmed that the only RZ-BMP and not the RZ-scBMP surfaces promote increased calcium deposition compared to TCP (Fig. S5†). Another possibility is that Alizarin red S staining is a rather unspecific measurement of osteogenic differentiation. In any case, when compared to the cell response on RZ-BMP proteins, cells on RZ-scBMP proteins did not enhance as many osteogenic markers. From these results, we conclude that the authentic BMP-2 peptide sequence elicits a more robust response compared to the scrambled sequence. Thus, the cells appear to respond to the RZ-BMP proteins in a sequence-specific manner.

Interestingly, it appeared that the RZ-BMP + RZ-scRGD proteins induced osteogenic differentiation similar to that of the RZ-BMP proteins. Specifically, the AP activity and calcium deposition were statistically equivalent between the two groups (Fig. 4 and 5, $p < 0.05$, Tukey's *post hoc* test). In addition, the RZ-BMP + RZ-scRGD proteins upregulated more osteogenic genes than the RZ-BMP proteins did. In particular, the RZ-BMP + RZ-scRGD surfaces upregulated the gene expression of Runx2 (day 7), AP (day 4), and type I col (day 4) (Fig. 6), whereas the RZ-BMP proteins did not. Overall, it appeared that the RZ-BMP and RZ-BMP + RZ-scRGD proteins both resulted in enhanced osteogenic differentiation compared to TCP.

We note that the density of the BMP-2 peptide was significantly lower on the RZ-BMP + RZ-scRGD surface than the RZ-BMP surface. In particular, the total amount of proteins was approximately equal on the RZ-BMP and RZ-BMP + RZ-scRGD surfaces (Fig. S1B†). But, because the RZ-BMP + RZ-scRGD protein surface is a 50 : 50 mixture, the BMP-2 peptide density on the RZ-BMP + RZ-scRGD surfaces is ~33 pmol cm^{-2}, which is almost half the density on the RZ-BMP proteins (69 pmol cm^{-2}). Taken together, these results suggest that peptide densities of 33–69 pmol cm^{-2} are sufficient to promote osteogenic differentiation and that, within this range, the density of the bioactive ligand (*i.e.*, the BMP-2 peptide sequence) did not significantly influence the extent of osteogenic differentiation. As a comparison, full-length BMP-2 growth factor immobilized on biomaterials promotes osteogenic differentiation at a density of 1.15–15.4 pmol cm^{-2},[43,44] which are lower than the density of the BMP-2 peptide in our study.

In our study, a combination of the BMP-2 peptide and RGD did not display synergistic effects on differentiation. In fact, it appeared as if the RZ-BMP + RZ-RGD surfaces were less potent

than either the RZ-BMP or RZ-BMP + RZ-scRGD surfaces in promoting osteogenic differentiation. Although the RZ-BMP + RZ-RGD surfaces did increase osteogenic gene expression (Fig. 6), the increased gene expression did not translate into higher AP activity or calcium deposition compared to TCP (Fig. 4 and 5). To verify these results, we confirmed that the amino acid sequences of the bioactive domains in the RZ-RGD and RZ-scRGD proteins were correct by analyzing both proteins through peptide sequencing (see Materials and methods for details).

Previous studies report conflicting results as to whether the BMP-2 peptide and the RGD cell-binding domain have a synergistic effect on osteogenic differentiation.[20,26,27,45] Some studies reported that when the RGD and BMP-2 peptides were grafted onto materials, higher osteogenic differentiation was observed compared to materials containing only the BMP-2 peptide.[20,27] Moore *et al.* investigated the effect of the concentration of both peptides on osteogenic differentiation and reported the synergistic enhancement on BSP expression only at a total concentration of 130 pmol cm^{-2} (*i.e.*, 65 pmol cm^{-2} for each peptide).[26] However, Koepsel *et al.* observed that the RGD and BMP-2 peptides did not have a significant effect on AP activity.[45] Potential reasons for the conflicting results regarding synergy could be due to differing peptide densities or modes of ligand presentation within the studies.

Last, given that the RZ-BMP + RZ-scRGD surface promoted osteogenic differentiation but the RZ-BMP + RZ-RGD surface did not, it appeared as if the presence of the RGD cell-binding domain suppressed the protein expression and calcium deposition elicited by the BMP-2 peptide sequence. There are several potential reasons that may contribute to this result. First, the RGD domain in the RZ-BMP + RZ-RGD surfaces may delay osteogenic differentiation due to strong cell adhesion to the surfaces. Previous studies demonstrate that RGD-modified materials resulted in a slower rate of osteogenesis than unmodified ones.[46,47] Second, when cells are cultured on the RZ-BMP + RZ-RGD surfaces, the enhanced osteogenic differentiation elicited by the BMP-2 peptide could be suppressed by integrin binding to the RGD domain. The RGD sequence, which is derived from fibronectin, interacts primarily with the $\alpha_v\beta_3$ and $\alpha_5\beta_1$ integrins,[48,49] which are expressed on the membrane of hMSCs[50,51] and human osteoblast-like cells.[52] In our study, it is likely that only the $\alpha_v\beta_3$ integrins bind the RGD domain in RZ-RGD because $\alpha_5\beta_1$ binding requires both the RGD sequence and the PHSRN synergy site found in fibronectin.[53] There are conflicting reports as to whether the $\alpha_v\beta_3$ integrins promote or suppress osteogenic differentiation.[54–59] However, some studies have observed that osteogenic differentiation was suppressed by $\alpha_v\beta_3$ integrin binding, and the inhibition was rescued by blocking the $\alpha_v\beta_3$ integrins.[55,57] In addition, RGD-functionalized surfaces that support $\alpha_v\beta_3$ binding retarded osteogenic differentiation.[58] Thus, it is possible that $\alpha_v\beta_3$ integrin binding to the RGD domain in RZ-RGD resulted in inhibition of osteogenic differentiation elicited by the BMP-2 peptide in RZ-BMP. However, further investigation is needed to identify the mechanism that contributes to the cell response observed on the RZ-BMP + RZ-RGD surface.

Taken together, our results demonstrate that the modular protein design provides a new strategy for incorporating the BMP-2 peptide in materials. We found that the BMP-2 peptide in modular proteins accelerated osteogenic differentiation of hMSCs and induced robust osteogenic differentiation in a sequence-specific manner.

Conclusions

This work successfully demonstrated a new strategy to incorporate the BMP-2 peptide in biomaterials for applications in bone tissue engineering. By using genetic engineering, a strategy that allows us to precisely control material properties, we incorporated the BMP-2 peptide into the backbone of our protein-based biomaterials. We found that, within the context of our modular proteins, the BMP-2 peptide was bioactive and accelerated osteogenic differentiation in a sequence-specific manner. In addition, our results showed that the density of the BMP-2 peptide (*i.e.*, 33 pmol cm^{-2} on RZ-BMP + RZ-scRGD or 69 pmol cm^{-2} on RZ-BMP) did not affect the extent of cell differentiation. Within the context of our modular proteins, the BMP-2 peptide did not synergize with the RGD cell-binding sequence. Overall, our results suggest that incorporation of bioactive peptides (the BMP-2 peptide in this study) into genetically-engineered proteins is a promising strategy for developing biomaterials for bone tissue engineering.

Acknowledgements

This work was supported by the Purdue School of Chemical Engineering and the College of Engineering), the National Science Foundation (Award No. 0927100-EEC and a Graduate Fellowship to J.N.R.), the American Heart Association Scientist Development Grant (12SDG8980014), and the 3M Nontenured Faculty Award. We thank Dr. Jo Davisson (Purdue University) for the kind gifts of *E. coli* expression host BL21-CodonPlus (DE3)-RIPL, Dr. David Tirrell (California Institute of Technology) for the pET28aRW plasmid, Victoria Hedrick and Dr. Lake Paul (Purdue Proteomics Facility) for conducting the amino acid analysis and peptide sequencing, Dr. Elizabeth Topp (Purdue University) for access to the CD spectroscopic instrument, and Dr. Jennifer Freeman (Purdue University) for access to her Nanodrop instrument. We thank the National Cancer Institute Biometric Research Branch Preclinical Repository for providing bFGF.

References

1 D. Sengupta and S. C. Heilshorn, *Tissue Eng., Part B*, 2010, **16**, 285–293.
2 S. Gomes, I. B. Leonor, J. F. Mano, R. L. Reis and D. L. Kaplan, *Prog. Polym. Sci.*, 2012, **37**, 1–17.

3 K. J. Lampe and S. C. Heilshorn, *Neurosci. Lett.*, 2012, **519**, 138–146.
4 D. L. Nettles, K. Kitaoka, N. A. Hanson, C. M. Flahiff, B. A. Mata, E. W. Hsu, A. Chilkoti and L. A. Setton, *Tissue Eng., Part A*, 2008, **14**, 1133–1140.
5 P. J. Nowatzki, C. Franck, S. A. Maskarinec, G. Ravichandran and D. A. Tirrell, *Macromolecules*, 2008, **41**, 1839–1845.
6 S. Ravi, C. A. Haller, R. E. Sallach and E. L. Chaikof, *Biomaterials*, 2012, **33**, 2431–2438.
7 L. Q. Li, Z. X. Tong, X. Q. Jia and K. L. Kiick, *Soft Matter*, 2013, **9**, 665–673.
8 S. Lv, D. M. Dudek, Y. Cao, M. M. Balamurali, J. Gosline and H. Li, *Nature*, 2010, **465**, 69–73.
9 J. N. Renner, K. M. Cherry, R. S. C. Su and J. C. Liu, *Biomacromolecules*, 2012, **13**, 3678–3685.
10 A. J. Mieszawska, L. D. Nadkarni, C. C. Perry and D. L. Kaplan, *Chem. Mater.*, 2010, **22**, 5780–5785.
11 S. Wohlrab, S. Müller, A. Schmidt, S. Neubauer, H. Kessler, A. Leal-Egaña and T. Scheibel, *Biomaterials*, 2012, **33**, 6650–6659.
12 J. C. Liu, S. C. Heilshorn and D. A. Tirrell, *Biomacromolecules*, 2004, **5**, 497–504.
13 J. C. Liu and D. A. Tirrell, *Biomacromolecules*, 2008, **9**, 2984–2988.
14 C. L. McGann, E. A. Levenson and K. L. Kiick, *Macromol. Chem. Phys.*, 2013, **214**, 203–213.
15 F.-M. Chen, M. Zhang and Z.-F. Wu, *Biomaterials*, 2010, **31**, 6279–6308.
16 M. F. Pittenger, A. M. Mackay, S. C. Beck, R. K. Jaiswal, R. Douglas, J. D. Mosca, M. A. Moorman, D. W. Simonetti, S. Craig and D. R. Marshak, *Science*, 1999, **284**, 143–147.
17 H. Senta, H. Park, E. Bergeron, O. Drevelle, D. Fong, E. Leblanc, F. Cabana, S. Roux, G. Grenier and N. Faucheux, *Cytokine Growth Factor Rev.*, 2009, **20**, 213–222.
18 A. Saito, Y. Suzuki, S. Ogata, C. Ohtsuki and M. Tanihara, *Biochim. Biophys. Acta*, 2003, **1651**, 60–67.
19 J. S. Lee, J. S. Lee and W. L. Murphy, *Acta Biomater.*, 2010, **6**, 21–28.
20 X. He, J. Ma and E. Jabbari, *Langmuir*, 2008, **24**, 12508–12516.
21 Z.-Y. Lin, Z.-X. Duan, X.-D. Guo, J.-F. Li, H.-W. Lu, Q.-X. Zheng, D.-P. Quan and S.-H. Yang, *J. Controlled Release*, 2010, **144**, 190–195.
22 A. Saito, Y. Suzuki, S. Ogata, C. Ohtsuki and M. Tanihara, *J. Biomed. Mater. Res., Part A*, 2004, **70A**, 115–121.
23 M.-J. Kim, B. Lee, K. Yang, J. Park, S. Jeon, S. H. Um, D.-I. Kim, S. G. Im and S.-W. Cho, *Biomaterials*, 2013, **34**, 7236–7246.
24 Y. Lu, J. S. Lee, B. Nemke, B. K. Graf, K. Royalty, R. Illgen, R. Vanderby, M. D. Markel and W. L. Murphy, *PLoS One*, 2012, **7**, e50378.
25 A. Saito, Y. Suzuki, M. Kitamura, S. I. Ogata, Y. Yoshihara, S. Masuda, C. Ohtsuki and M. Tanihara, *J. Biomed. Mater. Res., Part A*, 2006, **77A**, 700–706.
26 N. M. Moore, N. J. Lin, N. D. Gallant and M. L. Becker, *Acta Biomater.*, 2011, **7**, 2091–2100.
27 O. F. Zouani, C. Chollet, B. Guillotin and M. C. Durrieu, *Biomaterials*, 2010, **31**, 8245–8253.
28 J. N. Renner, Y. Kim, K. M. Cherry and J. C. Liu, *Protein Expression Purif.*, 2012, **82**, 90–96.
29 C. A. Gregory, W. Grady Gunn, A. Peister and D. J. Prockop, *Anal. Biochem.*, 2004, **329**, 77–84.
30 J. N. Renner, Y. Kim and J. C. Liu, *Tissue Eng., Part A*, 2012, **18**, 2581–2589.
31 G. E. P. Box and D. R. Cox, *J. R. Stat. Soc., Ser. B: Stat. Methodol.*, 1964, **26**, 211–252.
32 P. C. Bessa, M. Casal and R. L. Reis, *J. Tissue Eng. Regener. Med.*, 2008, **2**, 81–96.
33 P. C. Bessa, M. Casal and R. L. Reis, *J. Tissue Eng. Regener. Med.*, 2008, **2**, 1–13.
34 S. Long, L. Truong, K. Bennett, A. Phillips, F. Wong-Staal and H. Ma, *Protein Expression Purif.*, 2006, **46**, 374–378.
35 L. F. Vallejo, M. Brokelmann, S. Marten, S. Trappe, J. Cabrera-Crespo, A. Hoffmann, G. Gross, H. A. Weich and U. Rinas, *J. Biotechnol.*, 2002, **94**, 185–194.
36 Z. Haidar, R. Hamdy and M. Tabrizian, *Biotechnol. Lett.*, 2009, **31**, 1817–1824.
37 J. N. Zara, R. K. Siu, X. L. Zhang, J. Shen, R. Ngo, M. Lee, W. M. Li, M. Chiang, J. Chung, J. Kwak, B. M. Wu, K. Ting and C. Soo, *Tissue Eng., Part A*, 2011, **17**, 1389–1399.
38 A. Julka, A. S. Shah and B. S. Miller, *J. Shoulder Elbow Surg.*, 2012, **21**, E12–E16.
39 E. E. Golub and K. Boesze-Battaglia, *Curr. Opin. Orthop.*, 2007, **18**, 444–448.
40 Z. Li, Z. Zhou, M. M. Saunders and H. J. Donahue, *Am. J. Physiol. Cell Physiol.*, 2006, **290**, 1248–1255.
41 L. Zhao, M. Tang, M. D. Weir, M. S. Detamore and H. H. K. Xu, *Tissue Eng., Part A*, 2011, **17**, 969–979.
42 J. S. Lee, J. S. Lee, A. Wagoner-Johnson and W. L. Murphy, *Angew. Chem., Int. Ed.*, 2009, **121**, 6384–6387.
43 V. Karageorgiou, L. Meinel, S. Hofmann, A. Malhotra, V. Volloch and D. Kaplan, *J. Biomed. Mater. Res., Part A*, 2004, **71A**, 528–537.
44 Y. J. Park, K. H. Kim, J. Y. Lee, Y. Ku, S. J. Lee, B. M. Min and C. P. Chung, *Biotechnol. Appl. Biochem.*, 2006, **43**, 17–24.
45 J. T. Koepsel, P. T. Brown, S. G. Loveland, W. J. Li and W. L. Murphy, *J. Mater. Chem.*, 2012, **22**, 19474–19481.
46 H. L. Holtorf, J. A. Jansen and A. G. Mikos, *Biomaterials*, 2005, **26**, 6208–6216.
47 H. Shin, K. Zygourakis, M. C. Farach-Carson, M. J. Yaszemski and A. G. Mikos, *J. Biomed. Mater. Res., Part A*, 2004, **69A**, 535–543.
48 R. Pytela, M. D. Pierschbacher and E. Ruoslahti, *Proc. Natl. Acad. Sci. U. S. A.*, 1985, **82**, 5766–5770.
49 R. Pytela, M. D. Pierschbacher and E. Ruoslahti, *Cell*, 1985, **40**, 191–198.
50 J. E. Frith, R. J. Mills and J. J. Cooper-White, *J. Cell Sci.*, 2012, **125**, 317–327.
51 M. Majumdar, M. Keane-Moore, D. Buyaner, W. Hardy, M. Moorman, K. McIntosh and J. Mosca, *J. Biomed. Sci.*, 2003, **10**, 228–241.

52 S. Gronthos, K. Stewart, S. E. Graves, S. Hay and P. J. Simmons, *J. Bone Miner. Res.*, 1997, **12**, 1189–1197.
53 E. H. J. Danen, S.-i. Aota, A. A. van Kraats, K. M. Yamada, D. J. Ruiter and G. N. P. van Muijen, *J. Biol. Chem.*, 1995, **270**, 21612–21618.
54 S.-L. Cheng, C.-F. Lai, S. D. Blystone and L. V. Avioli, *J. Bone Miner. Res.*, 2001, **16**, 277–288.
55 B. G. Keselowsky, D. M. Collard and A. J. García, *Proc. Natl. Acad. Sci. U. S. A.*, 2005, **102**, 5953–5957.
56 C. F. Lai and S. L. Cheng, *J. Bone Miner. Res.*, 2005, **20**, 330–340.
57 M. M. Martino, M. Mochizuki, D. A. Rothenfluh, S. A. Rempel, J. A. Hubbell and T. H. Barker, *Biomaterials*, 2009, **30**, 1089–1097.
58 T. A. Petrie, J. E. Raynor, C. D. Reyes, K. L. Burns, D. M. Collard and A. J. García, *Biomaterials*, 2008, **29**, 2849–2857.
59 G. B. Schneider, R. Zaharias and C. Stanford, *J. Dent. Res.*, 2001, **80**, 1540–1544.